

A COMPACT DUAL-BAND POWER DIVIDER USING PLANAR ARTIFICIAL TRANSMISSION LINES FOR GSM/DCS APPLICATIONS

T. Yang, C. Liu, L. Yan, and K. Huang

School of Electronics and Information Engineering
Sichuan University
Chengdu 610064, China

Abstract—A compact dual-band power divider for GSM/DCS applications is proposed in this letter. Novel planar artificial transmission lines are applied to miniaturize the power divider and achieve wideband response. The proposed dual-band power divider is about 37% of conventional one. The design principle, simulated and measured results are all discussed. The measured results show that good performance can be achieved at the operation frequencies.

1. INTRODUCTION

Power dividers are widely used in microwave and mm-wave circuits, such as antenna arrays, power amplifiers, mixers, and etc. There are many types of power dividers for various applications [1–4]. In recent years, due to the multi-band requirements, various dual-band power dividers have been reported, e.g., placing an open or short stub nearby the input [5] or in the middle of the transmission line [6], adding extra lumped inductor and capacitor in parallel with the isolation resistor [7]. But those topologies are not compact enough using conventional microstrip transmission lines. Meanwhile, spurious responses may be introduced at some harmonic frequencies.

In this letter, a compact dual-band power divider using novel planar artificial transmission lines is presented. A dual-band power divider operating at frequency f_0 and $2f_0$ for GSM/DCS applications is fabricated and measured to verify the design. A lumped inductor and a lumped capacitor are placed in parallel with the isolation resistor in the power divider.

Corresponding author: C. Liu (cjliu@ieee.org).

2. PRINCIPLE

2.1. The Planar Artificial Transmission Line

For miniaturization of conventional transmission lines, various techniques have been reported. Recently, a novel planar artificial transmission line was proposed [8,9]. It is composed of microstrip quasi-lumped elements and their discontinuities with single-layer printed circuit board. It can easily synthesize transmission lines with a wide range of characteristic impedances and electrical lengths. The required physical lengths of both high- and low-impedance microstrip lines can be greatly reduced, especially in low frequency range.

The unit cell of the artificial transmission line and its corresponding equivalent lumped circuit model are shown in Figs. 1(a) and (b), respectively. Referring to the circuit model in Fig. 1(b), the inductors L_1 , L_2 , L_3 represent meandered-line inductors, while the C_{11} , C_{12} , C_{13} , C_{14} represent the parasitic capacitance of the meandered-line inductors L_1 , L_3 . The capacitors C_1 and C_2 are

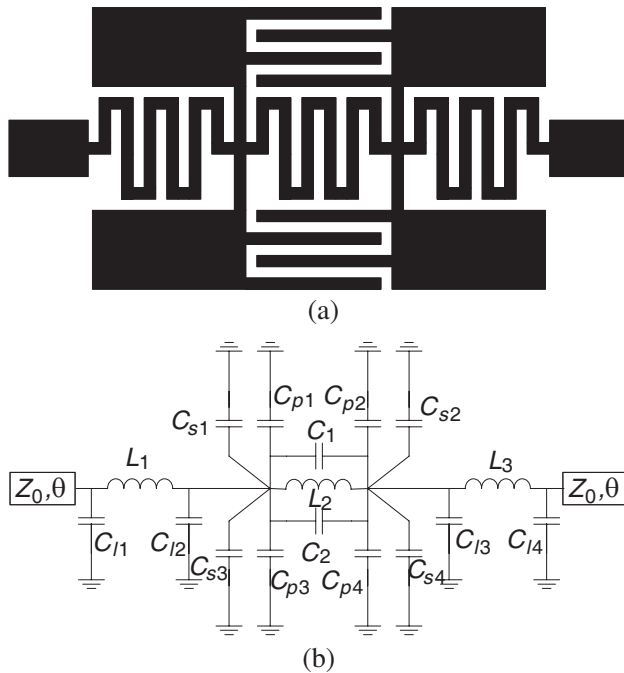


Figure 1. Unit cell of the artificial transmission line. (a) Circuit layout. (b) Equivalent lumped circuit model.

realized by two interdigital capacitors. C_{p1} , C_{p2} , C_{p3} , C_{p4} represent the parasitic capacitors caused by meandered-line inductor L_2 and the two interdigital capacitors. The shunt capacitors C_{s1} , C_{s2} , C_{s3} , C_{s4} are realized by four microstrip parallel-plated capacitors. The characteristic impedance Z_c and guided wavenumber β_g of the artificial transmission line can be given by [8]

$$Z_c = \sqrt{L_{\text{tot}}/C_{\text{tot}}} \quad (1)$$

$$\beta_g = \omega \sqrt{L_{\text{tot}} \cdot C_{\text{tot}}} \quad (2)$$

where L_{tot} and C_{tot} represent the total equivalent inductance and capacitance of the artificial transmission line, respectively. L_{tot} and C_{tot} can be obtained from the equivalent circuit model.

According to (1), (2), it is apparent to verify that, as L_{tot} and C_{tot} rise proportionally, the guided wavenumber increases, whereas the characteristic impedance remains unchanged. So it can effectively reduce the required physical length of a microstrip line by reducing the guided wavelength λ_g with the given characteristic impedance and electrical length. Compact components can be designed based on this characteristic.

Moreover, another important characteristic is that, the parallel resonant LC-tank inserted in the middle stage of the artificial transmission line may introduce multiple finite-frequency transmission zeroes at the high frequency range. Hence the artificial transmission line has the ability of suppressing spurious harmonic responses in various circuits, and can give good broadband responses over a very wide frequency range.

2.2. The Dual-Band Power Divider Scheme

The dual-band power divider operation scheme has been proposed using two section impedance transformers and a parallel RLC circuit [7]. The schematic diagram is shown in Fig. 2.

Within the scheme, the power divider can realize the power division both at the fundamental frequency f_0 and its first harmonic frequency $2f_0$.

With the odd- and even-mode analysis, the circuit parameters can be determined as [7]

$$Z_2 = 1.26Z_0, \quad Z_1 = 1.59Z_0 \quad (3)$$

$$L = \frac{0.282Z_0}{f_0}, \quad C = \frac{0.045}{f_0Z_0} \quad (4)$$

$$R = 2Z_0 \quad (5)$$

For the operating frequency at 900 MHz, in a system $Z_0 = 50 \text{ Ohm}$, these parameters are: $Z_1 = 79.5 \text{ Ohm}$, $Z_2 = 63 \text{ Ohm}$, $L = 15.67 \text{ nH}$, $C = 1.0 \text{ pF}$, $R = 100 \text{ Ohm}$.

3. DESIGN AND MEASUREMENT

For GSM/DCS applications, the center frequencies are 900 MHz and 1800 MHz, the design parameters can be obtained by solving (3)–(5). And according to (1), (2), artificial transmission lines can be designed for desired characteristic impedance. A compact dual-band power divider is designed and realized on a substrate ($\epsilon_r = 2.65$, $h = 1 \text{ mm}$). A photograph of the fabricated power divider is shown in Fig. 3.

The overall size of the circuit is $49 \text{ mm} \times 23 \text{ mm}$ or equivalently, $0.2\lambda_g \times 0.1\lambda_g$. λ_g here is the guided wavelength at 900 MHz. $l_1 = 14.4 \text{ mm}$, $l_2 = 13.5 \text{ mm}$ and the exact parameters of the lumped components are: $L = 15 \text{ nH}$, $C = 1.0 \text{ pF}$, $R = 100 \text{ Ohm}$.

The proposed design was measured using an Agilent N5230A

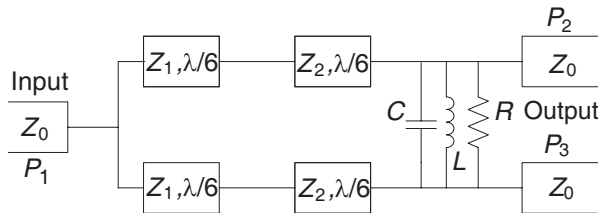


Figure 2. Dual-band power divider schematic diagram.

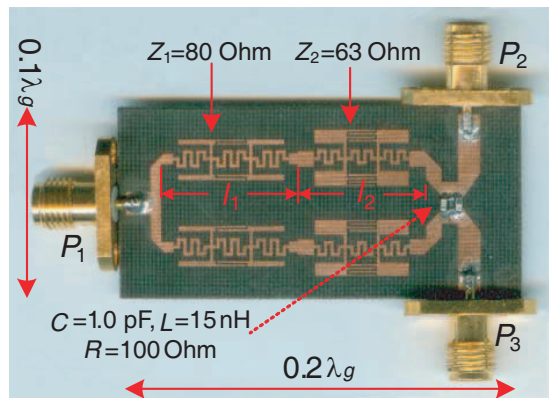


Figure 3. Photograph of the fabricated dual-band power divider.

vector network analyzer. Simulation results of the power divider are from IE3D. The simulated and measured S -parameters of the design are illustrated in Fig. 4. Measured results show a good agreement with simulations.

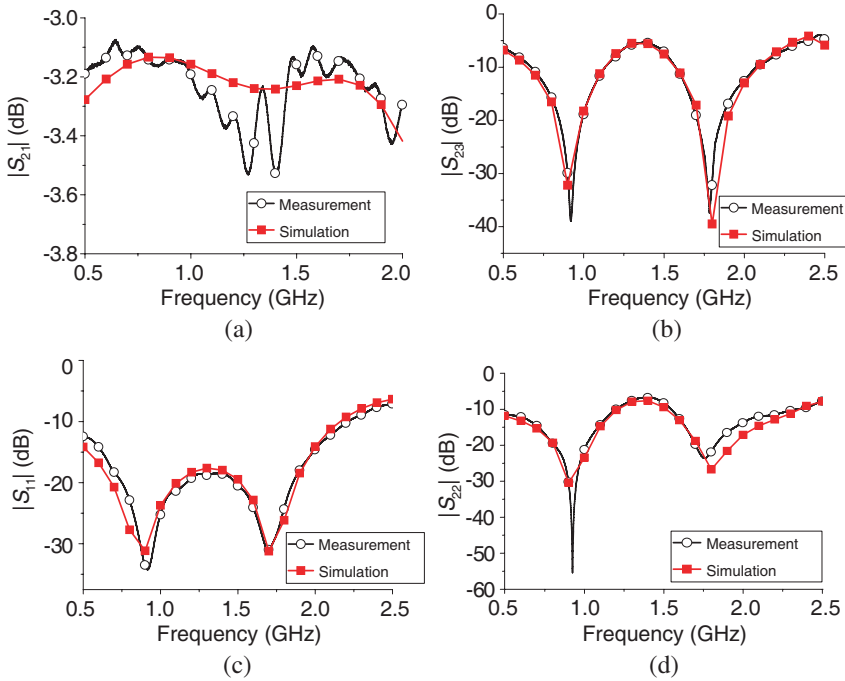


Figure 4. Simulation and measurement results of S -parameters. (a) Magnitude of S_{21} . (b) Magnitude of S_{23} . (c) Magnitude of S_{11} . (d) Magnitude of S_{22} .

The performance of the proposed design is excellent. As shown in Figs. 4(a), (b), (c) and (d), at the operation frequency of 900 MHz: $|S_{21}| = -3.14$ dB, $|S_{23}| = -32.02$ dB, $|S_{11}| = -33.64$ dB, $|S_{22}| = -30.4$ dB; at the other operation frequency of 1800 MHz: $|S_{21}| = -3.21$ dB, $|S_{23}| = -31.2$ dB, $|S_{11}| = -24.06$ dB, $|S_{22}| = -21.7$ dB. Good balance can be achieved between the two output ports according to Fig. 5. The magnitude difference between two output ports is 0.21 dB at 900 MHz and 0.22 dB at 1800 MHz, while the phase difference is 1.78° at 900 MHz and 2.3° at 1800 MHz. The wideband response is shown in Fig. 6. The attenuation is greater than 20 dB from 3.7 GHz to 10 GHz (even much higher frequency). It shows that the artificial transmission line used in the design can effectively suppress the harmonic response.

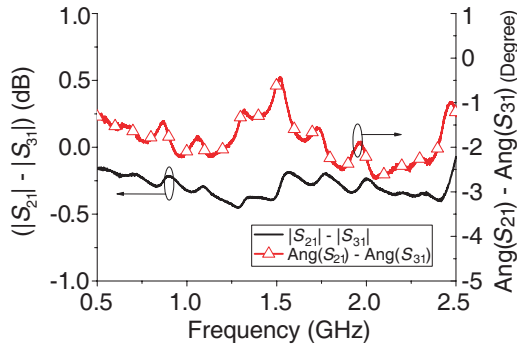


Figure 5. Magnitude and phase differences between S_{21} and S_{31} .

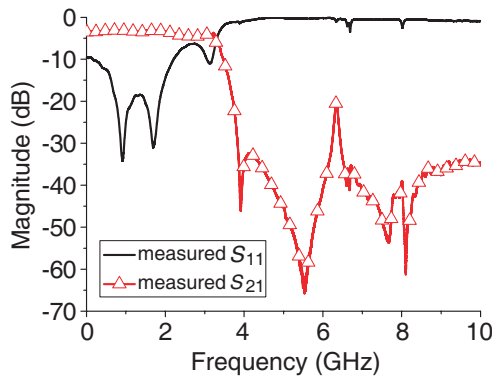


Figure 6. Wideband response of the power divider.

4. CONCLUSION

In this letter, a novel dual-band frequency power divider for GSM/DCS applications has been presented. By introducing artificial transmission lines, the proposed power divider is of $0.2\lambda_g$ by $0.1\lambda_g$, which is about 37% of conventional microstrip dual-band frequency power divider. It is with good return loss, insertion loss and isolation. In addition, the wideband response of the power divider is excellent. The simulations show a good agreement with the measured results.

REFERENCES

1. Chen, H. and Y. Zhang, "A novel compact planar six-way power divider using folded and hybrid-expanded coupled lines," *Progress*

- In Electromagnetics Research*, PIER 76, 243–252, 2007.
2. Oraizi, H. and M. S. Esfahlan, “Miniaturization of Wilkinson power dividers by using defected ground structures,” *Progress In Electromagnetics Research Letters*, Vol. 4, 113–120, 2008.
 3. Fan, F., Z. Yan, and J. Jiang, “Design of a novel compact power divider with harmonic suppression,” *Progress In Electromagnetics Research Letters*, Vol. 5, 151–157, 2008.
 4. Shamsinejad, S., M. Soleimani, and N. Komjani, “Novel miniaturized Wilkinson power divider for 3G mobile receivers,” *Progress In Electromagnetics Research Letters*, Vol. 3, 9–16, 2008.
 5. Cheng, K.-M. and F.-L. Wong, “A new Wilkinson power divider design for dual band application,” *IEEE Microwave Wireless Components Letters*, Vol. 17, 664–666, September 2007.
 6. Park, M.-J. and B. Lee, “A dual-band wilkinson power divider,” *IEEE Microwave Wireless Components Letters*, Vol. 18, 85–87, February 2008.
 7. Wu, L., H. Yilmaz, T. Bitzer, and A. P. M. Berroth, “A dual-frequency Wilkinson power divider: For a frequency and its first harmonic,” *IEEE Microwave Wireless Components Letters*, Vol. 15, 107–109, February 2005.
 8. Wang, C.-W., T.-G. Ma, and C.-F. Yang, “A new planar artificial transmission line and its applications to a miniaturized butler matrix,” *IEEE Trans. Microwave Theory Tech.*, Vol. 55, 2792–2801, December 2007.
 9. Wang, C.-W., T.-G. Ma, and C. -F. Yang, “Miniaturized branch-line coupler with harmonic suppression for RFID applications using artificial transmission lines,” *IEEE MTT-S Int. Microwave Symp. Dig.*, 29–32, June 2007.